

Microstructural Changes in the Reduction of Pr-123 with Lithium

A. Várez,* E. Morán,† and M. A. Alario-Franco^{1,†}

*Departamento Ingeniería E. Politécnico Superior, Universidad Carlos III, 28913 Leganés, Madrid, Spain, and

†Departamento de Química Inorgánica, Facultad de Ciencias Químicas, Universidad Complutense, 28040 Madrid, Spain

Received November 22, 1993; accepted January 20, 1994

IN HONOR OF C. N. R. RAO ON HIS 60TH BIRTHDAY

The microstructural changes produced in the reaction of *n*-butyl-lithium with PrBa₂Cu₃O₇ have been followed by means of high resolution electron microscopy and electron diffraction. Extended defects are produced which have been interpreted on the basis of the Pr-124 structure. Although obtained in a disordered form, this is the first report on the pure, i.e., yttrium free PrBa₂Cu₄O₈ structure. © 1994 Academic Press, Inc.

EXPERIMENTAL

Ba₂PrCu₃O₇ was prepared by the standard ceramic method from CuO, BaCuO₃, and Pr₂CuO₄; the last was obtained by the solid state reaction between Pr₆O₁₁ and CuO (9). Mixed powders were heated in air at 950°C for 24 hr, subsequently annealed in an oxygen atmosphere at 500°C for 6 hr, and slowly cooled down to room temperature.

The reaction of Ba₂PrCu₃O₇ with *n*-BuLi was carried out following Refs. (10–12).

The amount of lithium was approximately evaluated by the reaction of the lithiated material with an iodine solution in acetonitrile. The amount of reacted iodine was determined by titration with a standard thiosulphate solution.

X-ray diffraction experiments were performed on a Siemens D-5000 diffractometer with a graphite monochromator and CuK α radiation. Structural refinements have been done by means of the Rietveld method (13) using the Fullproff program (14).

Electron diffraction and microscopy were carried out in a JEOL 2000 FX TEMSCAN analytical electron microscopy operating at 200 kV; high resolution electron microscopy (HREM) was performed in a Jeol 4000 EX instrument working at 400 kV.

RESULTS AND DISCUSSION

1. X-ray Data

The as prepared Pr-123 was a well crystallized material but difficult to obtain free from the very stable perovskite BaPrO₃, whose most intense line, $d_{200} \sim 3.2086$ Å, often appeared although with a small intensity (see Fig. 1 a). This may, in fact, be due to the decomposition of Pr-123; see below. The lattice parameters appear in Table 1 and the relatively long cell parameters observed seem to indicate that the sample is well oxygenated.

INTRODUCTION

Very early in the development of the TRBa₂Cu₃O₇ compounds, it was realized that the praseodymium member of the family was exceptional in being tetragonal and non-superconducting while most other members were orthorhombic and superconducting at temperatures above the B.P. of nitrogen at atmospheric pressure (1, 2). In fact, PrBa₂Cu₃O₇ was not even metallic (3). The determination of the crystal structure of Pr-123 (4) showed that the origin of the tetragonality resided in the equal half occupation of the basal plane's oxygen positions. Although this is by no means an explanation of the lack of superconductivity in this material it is very likely related to it.

Recently, we have followed the process of reduction of YBa₂Cu₃O₇ with *n*-butyl-lithium (*n*-BuLi, in what follows). In this process, new phases, belonging to the Y₂Ba₄Cu_{6+n}O_{14+n} family, have appeared (5, 6), and lithium ionic conductors have been prepared and studied (7). It was then considered interesting to study the reaction of PrBa₂Cu₃O₇ with *n*-BuLi in order to see whether parallel behaviour could be observed (8) and to check possible changes in the magnetic properties produced by these means. In the course of the lithium reduction, although no significant changes in the magnetic properties—which will be described elsewhere—are produced, important microstructural changes are observed. These are described here.

¹ To whom correspondence should be addressed.

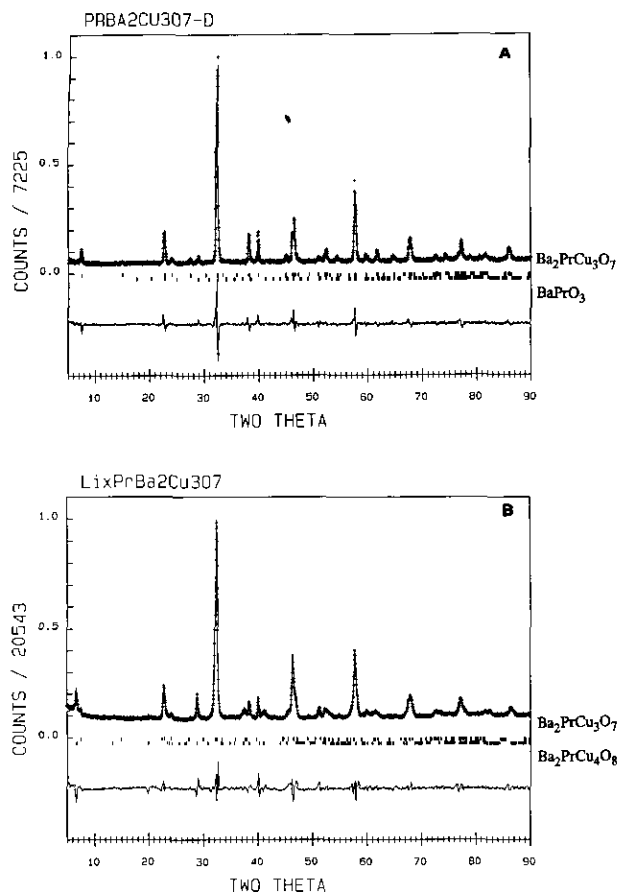


FIG. 1. XRD patterns ($\text{CuK}\alpha$) corresponding to samples of nominal composition. (a) $\text{Ba}_2\text{PrCu}_3\text{O}_7$ and (b) $\text{Li}_{0.26}\text{Ba}_2\text{PrCu}_3\text{O}_7$. Peaks marked as \blacktriangle correspond to the internal standard.

The lithiated materials show different *behavior* depending on their *nominal* lithium content:

For low Li content, i.e., $\text{Li/Pr} \approx .26$, there appear no qualitative changes in the X-ray patterns, and the cell parameters remain practically constant (Table 1).

For a higher ratio, $\text{Li/Pr} > .26$, besides a decrease in the signal to background ratio and a slight increase in the peak width, an increase in the unit cell volume was observed; this was essentially due to an increase in the c -

axis length. Upon delithiation these changes are reversed (Table 1). Also, a new diffraction maximum at low angle, $d \sim 13.1$ Å, was observed.

Following our early work on the Li reduction of Y-123 (5, 6), the presence of this maximum could be attributed to the formation of a 124-type phase (see Fig. 1-b). However, such phase has not yet been prepared in the Pr–Ba–Cu–O₂ system, where, up to now, the richest Pr containing phase so far prepared in the solid solution $\text{Pr}_x\text{Y}_{1-x}\text{Ba}_2\text{Cu}_4\text{O}_{7-\delta}$, corresponds to $x \sim .8$ (15). A closer look at the microscopic level of the reduction products was considered mandatory.

2. Electron Microscopy Results

Medium resolution study. Figure 2 shows three electron diffraction patterns corresponding to a typical crystal of the more lithiated Pr-123, nominal composition $\text{Li}_{0.26}\text{PrBa}_2\text{Cu}_3\text{O}_7$. The first one, which on the basis of the Pr-123 cell can be indexed as zone axis [021], shows a certain arcing of the spots indicative of a somewhat poor crystallinity, thus confirming the X-ray diffraction results. The other two diagrams, zone axis [110] and [010], clearly show streaking along the c^* -axis, thus indicating the presence of defects/disorder along c in the real crystal.

Figure 3 shows an electron micrograph corresponding to the last orientation; the presence of many extended defects, consisting of white bands each limited by two dark fringes, is obvious. Between these defects, it is possible to distinguish the $d_{001} \sim 11.8$ Å fringes of the Pr-123 cell, to which the extended defects are parallel. The fine structure of the defects shows a kind of "mottled contrast," also observed by Wada *et al.* (16), in the degradation of Y-123 in air. We will describe below the origin of this contrast, which is obviously related to the structure of the defects. It is also worth noting that some of the defects do not run across the whole crystal, as if they had grown from the edge and stopped before completion. It is also quite obvious that this reaction product is rather heterogeneous, some defect-rich regions coexisting, within the same crystal, with defect-free zones.

TABLE 1
Unit Cell Parameters Corresponding to the "Fresh," Lithiated and Delithiated Ba–Pr–Cu 123 Materials

Li/Pr	Lithiated			Delithiated		
	$a = b$ (Å)	c (Å)	V (Å ³)	$a = b$ (Å)	c (Å)	(Å ³)
0	3.9076(3)	11.8335(9)	180.69(4)	—	—	—
0.12	3.9090(3)	11.833(1)	180.81(4)	3.9089(2)	11.8366(6)	180.86(3)
0.21	3.9061(2)	11.8334(9)	180.55(3)	3.9107(1)	11.8386(5)	181.05(2)
0.26*	3.9049(2)	12.006(6)	183.1(1)	3.9182(7)	11.698(3)	179.7(1)

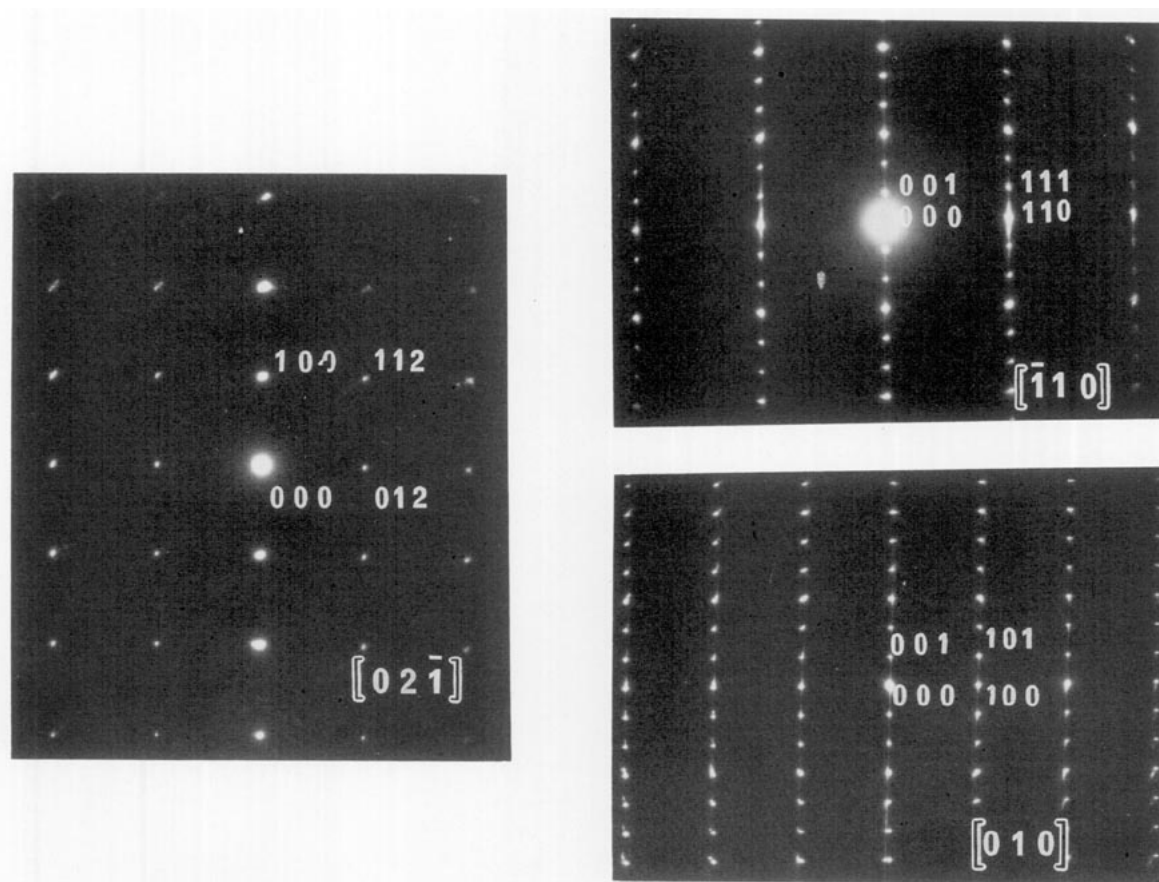


FIG. 2. Electron diffraction patterns of the $\text{Li}_{1.26}\text{Ba}_2\text{PrCu}_3\text{O}_7$ sample along the $[02\bar{1}]$, $[\bar{1}10]$, and $[010]$ zone axes. Streaking along the c^* axis is apparent.

High resolution study. Figure 4 shows a crystal of the same highly lithiated sample, nominal composition " $\text{Li}_{1.26}\text{PrBa}_2\text{Cu}_3\text{O}_{7-\delta}$." The zone axis, as determined from the electron diffraction pattern, is $[010]/[100]$; also, streaking is again apparent along the c -axis. In this crystal, two different regions can clearly be distinguished.

At higher magnification, Fig. 5a, the Ba-Pr-Ba sequence is prominent in the most regular part of the crystal, and the projections of the *single* copper-oxygen planes, which constitute the basal planes characteristic of the 123 structure, are clearly visible, Figure 5b. Image simulations of the Pr-123 structure do indeed confirm this assignment (8).

The rest of the crystal is, however, very disordered, and several features are worthy of note. To get a clear understanding of these features, it is important to briefly consider the so-called 124 structure (17) which, belonging to the family $\text{TR}_2\text{Ba}_4\text{Cu}_{6+n}\text{O}_{14+n+\delta}$, is characterized by a double copper-oxygen plane between every two barium planes, Figs. 5a and 5b. The presence of these two copper-oxygen planes gives an orthorhombic cell with two very different projections along $[100]$, Fig. 5a, and $[010]$, Figure 5b. In the first case, the two copper atoms of the

double copper-oxygen plane are mutually displaced by the translation $\frac{1}{2}[011]$, while, when viewed along $[010]$, they appear related by a *pseudomirror* plane parallel to (001) . Also, due to the presence of the double plane, the c -axis of the unit cell is more than twice (~ 27.6 Å) that of the 123 structure (~ 11.3 Å). Image simulations (8) indicate that, by electron microscopy, these two projections can easily be distinguished.

In the disordered crystal region, there are no less than 10 defects, essentially consisting of double Cu-O planes (these are marked by arrows). From both the Ba-Pr-Ba sequences and the Ba-Ba projected separation, it is a simple matter to differentiate whether the double Cu-O plane, i.e., the portion of the Pr-124 structure, is oriented along $[010]$, as in regions marked AA, or along $[100]$, as in the regions marked BB in Figure 7a. In the light of the present HREM information, the origin of the so-called "mottled contrast" (16) can be traced back to the presence of the double tunnels that the 124-type structure shows in the $[010]$ projection, Fig. 6b. In any case, the HREM pictures allow the structure of these defects to be established. It consists of a double copper-oxygen plane, the white region in Fig. 3, separating two barium-oxygen



FIG. 3. Transmission electron micrograph of the $\text{Li}_{.26}\text{Ba}_2\text{PrCu}_3\text{O}_7$ sample taken along the [010] zone axis. Extended defects perpendicular to the c^* axis of the 123 matrix are clearly observed.

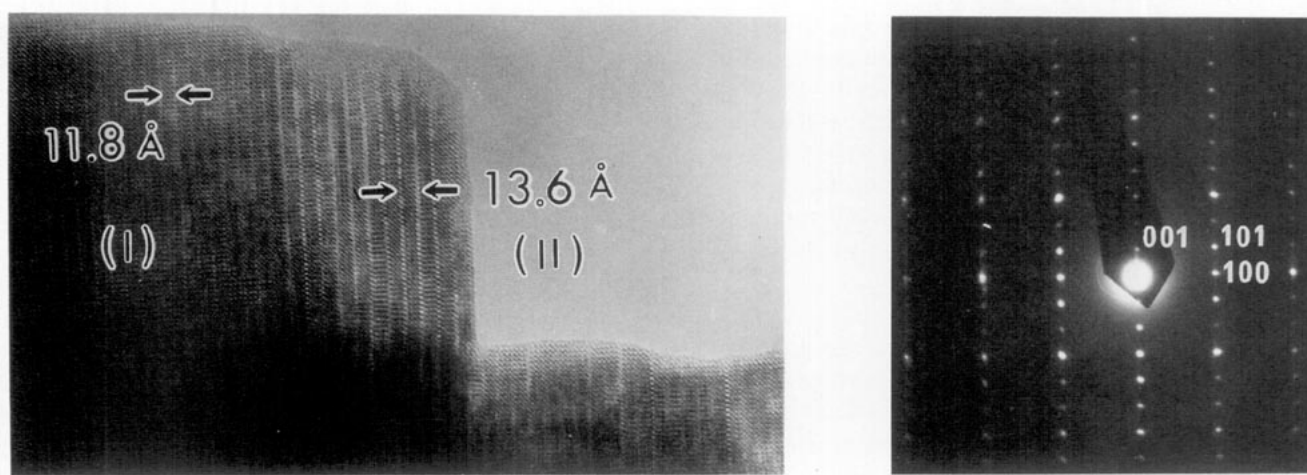


FIG. 4. (a) High resolution electron micrograph of the $\text{Li}_{.26}\text{Ba}_2\text{PrCu}_3\text{O}_7$ sample taken along the [100] zone axis. Two different regions are apparent: the original 123 structure labeled as (I) and the 124 one, produced upon lithiation, labeled (II). (b) Electron diffraction pattern corresponding to the HREM image.

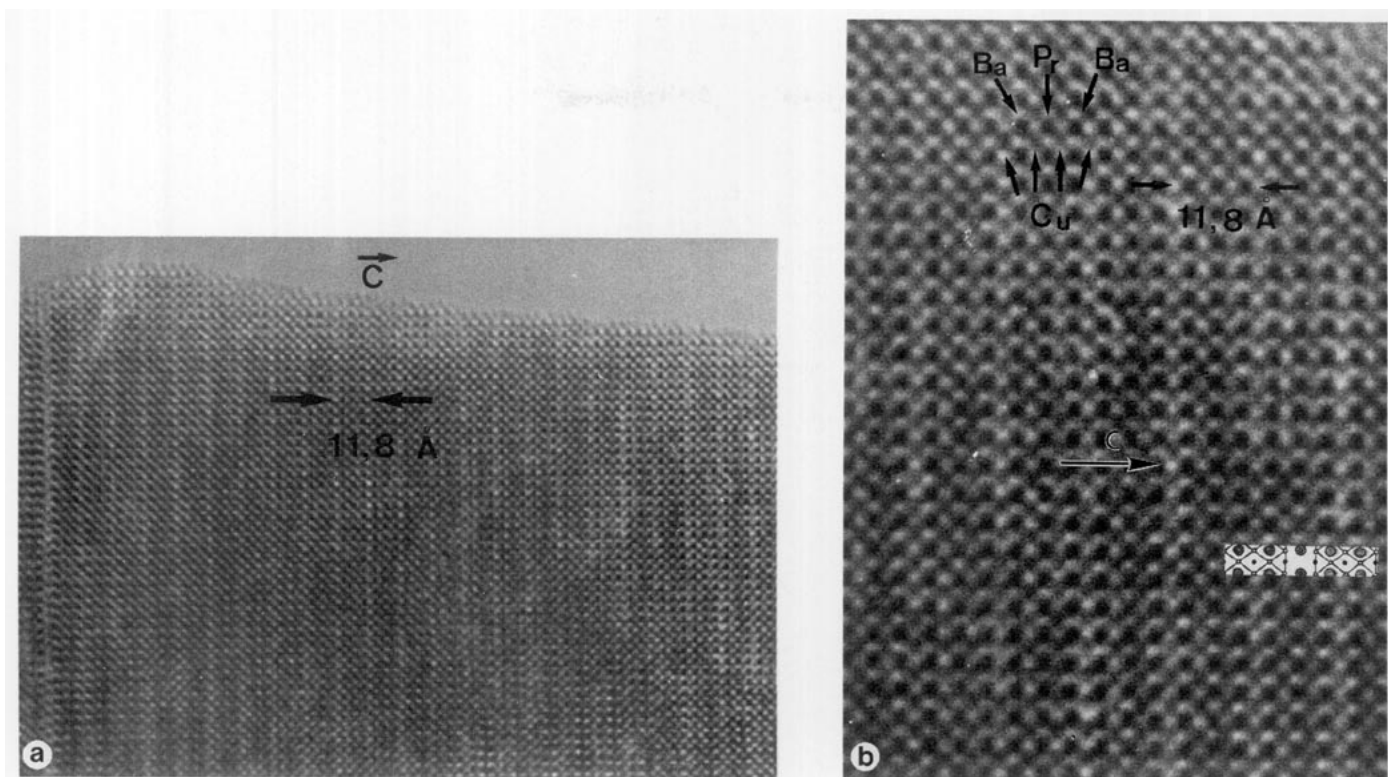


FIG. 5. (a) HREM image of the defect-free part of the $\text{Li}_{1.26}\text{Ba}_7\text{PrCu}_3\text{O}_7$ sample observed along $[100]$ (zone I of Fig. 4a). (b) Enlargement of the same area. The sequence Ba-Pr-Ba and the single copper-oxygen planes are clearly apparent. Two unit cells are schematized in the inserts.

planes which, at low resolution, originate the two dark lines seen there.

However, the disorder present in this crystal is more complicated than those simple defects:

On the one hand, some double Cu-O planes change

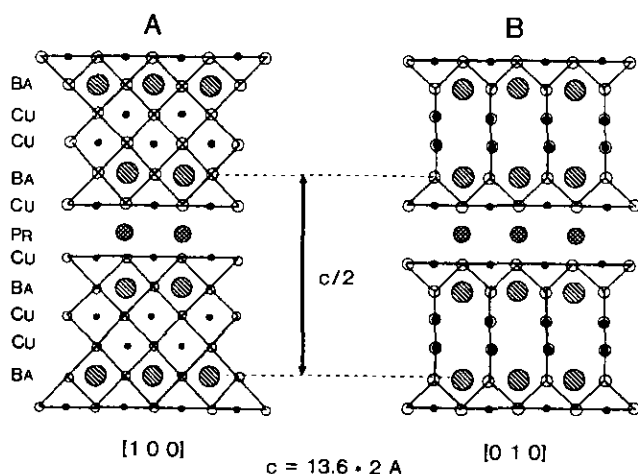


FIG. 6. Schematic illustration of the 124 structure looking (a) parallel to the $[100]$ direction, where the double $[\text{CuO}_4]$ chains are displaced by a translation of $\frac{1}{2} [011]$, and (b) parallel to the $[010]$ direction where the copper atoms of the double chains are related by a (011) pseudomirror plane.

orientation from $[010]$ to $[100]$ along the defect, as in region BA in Fig. 7a. But there are also other crystal regions where some of the Ba atoms are missing and what appears to resemble a triple Cu-O plane is apparent.

On the other hand, although the top edge of this crystal is covered by an amorphous skin, which extends along the rounded top right corner, the right, vertical edge shows clearly the presence of two unit cells from the pristine Pr-123 structure. Further, this crystal region ends up at that edge by a Cu-O plane. This is most interesting, since it is usually assumed that the 123 material offers a Ba or RE surface, which easily gets carbonated or hydrated.

It is, however, much more difficult to establish unambiguously how Pr-123 transforms to Pr-124 in the presence of lithium; in other words, it is difficult to establish the reduction mechanism. Bearing in mind that the process takes place in solution, two likely possibilities appear. The first would consist in the dissolution of the part of the structure included within a Ba-Y-Ba sequence; this will place two Cu-O basal planes together and this would eventually merge in the 124-type structure. The other possibility consists in the introduction of an extra copper-oxygen layer between a Ba-O plane and a Cu-O one. This will take place from the crystal edge toward its interior.

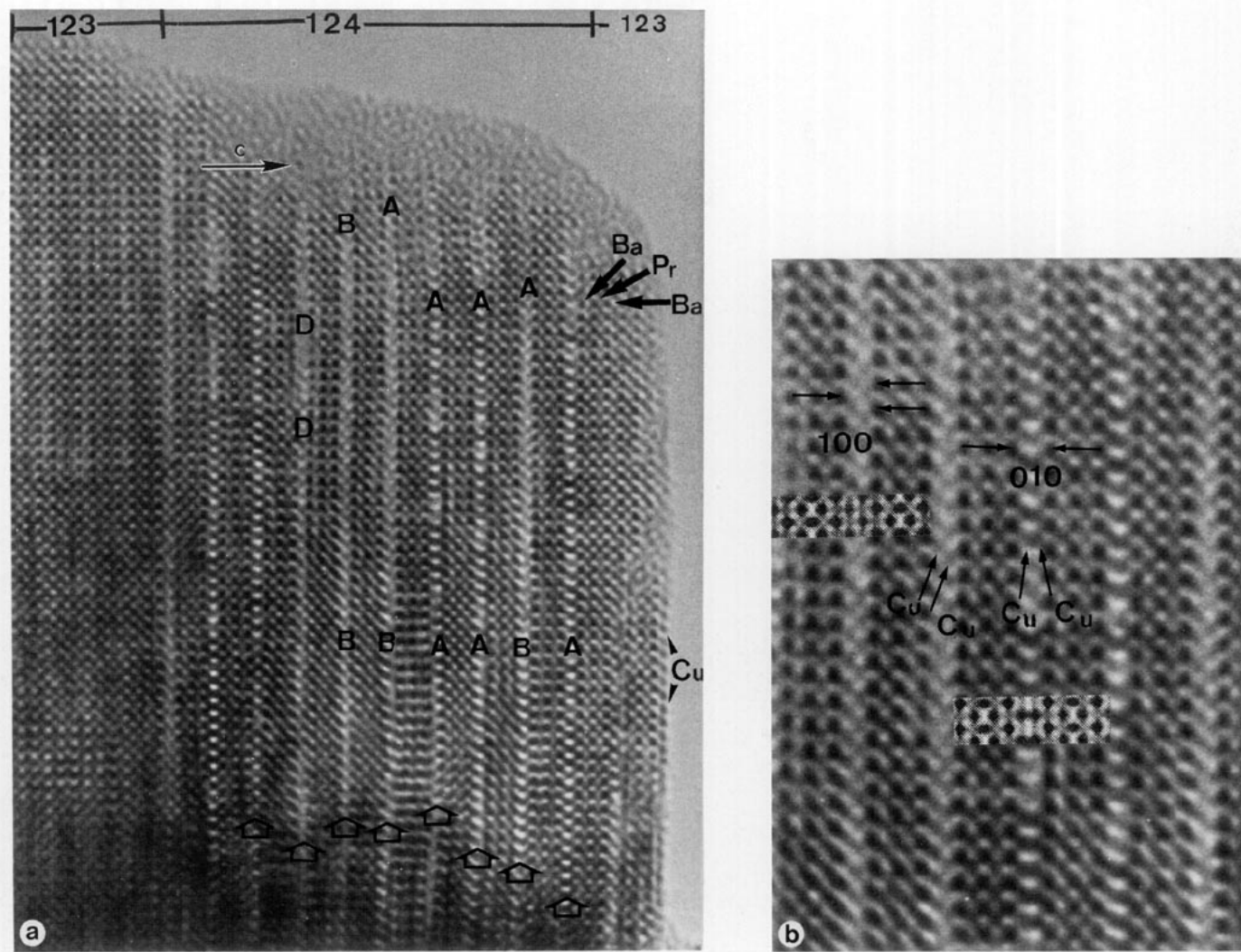


FIG. 7. (a) HREM image of the disordered area labeled (II) in Fig. 4a. Different regions (see text) and a very clean copper–oxygen surface can be observed. (b) Enlargement of the same area, where the twinned nature of the 124 phase is shown. Inserts correspond to calculated images.

It is difficult to select one of these two possibilities, and, indeed, there may be many others. Yet the evidence shown above, and in particular the fact that some of the extended defects that eventually grow up the 124-type phase do in fact start at the crystal edge and run towards the interior of the crystal (cf. Fig. 3), would seem to indicate that the second model is somewhat more likely. However, how the copper and oxygen atoms arrive at the nucleation point for the defect to grow remains a mystery.

It is perhaps worth noting that most of the crystal area shown in Fig. 7b corresponds to the new phase $\text{PrBa}_2\text{Cu}_4\text{O}_x$. Unfortunately, by this procedure it is impossible to obtain it in a pure form, the major impurities obtained being the very stable BaPrO_3 perovskite and lithium, which from its ionic conductivity properties would appear to behave as in the lithium tungsten bronzes (8).

ACKNOWLEDGMENTS

We gratefully acknowledge financial support from CICYT (Projects MAT 89/0768 and MAT 0374/92) and the Midas program, which also provided a grant to A.V.A. We also thank Fundación Domingo Martínez and Fundación Areces for research awards. We are grateful to our colleagues, M. A. Señaris-Rodríguez and C. J. D. Hetherington, for fruitful discussions and to Angel Landa-Cánovas and the Electron Microscopy Center of our University, in particular Juan-Luis Baldonado, for technical help.

REFERENCES

1. L. Sodelhorm, K. Zhang, D. G. Hinks, M. A. Beno, J. D. Jorgensen, C. U. Sergré, and I. K. Schuller, *Nature* **328**, 604 (1987).
2. M. K. Wu, J. R. Ashborn, C. J. Torng, P. H. Hor, R. L. Meng, L. Gao, Z. J. Huang, Y. Q. Wang, and C. W. Chu, *Phys. Rev. Lett.* **58**, 908 (1987).

3. J. L. Peng, P. Klavins, R. N. Shelton, H. B. Radowsky, P. H. Hahn, and L. Bernárdez, *Phys. Rev. B* **40**, 4517 (1989).
4. E. Morán, U. Amador, M. Barahona, M. A. Alario-Franco, A. Vegas, and J. Rodríguez-Carvajal, *Solid State Commun.* **67**, 369 (1988).
5. M. A. Señaris-Rodríguez, C. J. D. Hetherington, A. Várez, E. Morán, and M. A. Alario-Franco, *J. Solid State Chem.* **95**, 388 (1991).
6. M. A. Señaris-Rodríguez, A. M. Chippindale, A. Várez, E. Morán, and M. A. Alario-Franco, *Physica C* **172**, 477 (1991).
7. A. Várez, E. Morán, M. A. Alario-Franco, J. Santamaría, G. González-Díaz, and F. Sánchez-Quesada, *Solid State Commun.* **76**, 917 (1990).
8. A. Várez, Doctoral Thesis. Universidad Complutense, Madrid (1993).
9. R. Saez-Puche, M. Norton, T. R. White, and W. S. Glausinger, *J. Solid State Chem.* **50**, 281 (1983).
10. M. B. Dines, *Mater. Res. Bull.* **10**, 287 (1975).
11. D. W. Murphy, F. J. Di Salvo, G. W. Hull, and J. V. Waszczak, *Inorg. Chem.* **15**, 17 (1976).
12. M. A. Alario-Franco, E. Moran, A. Várez, J. Santamaría, and F. Sánchez-Quesada, *Solid State Ionics* **44**, 73 (1990).
13. H. M. Rietveld, *J. Appl. Crystallogr.* **2**, 65 (1969).
14. J. Rodríguez-Carvajal, "FULLPROF Program: Rietveld Pattern Matching Analysis of Powder Patterns." Grenoble, IL (1990).
15. P. Berástegui, L. G. Johansson, M. Kall, and L. Borjesson, *Physica C* **204**, 147 (1992).
16. O. Wada, T. Odaka, M. Wakata, T. Ogama, and A. Yosidome, *J. Appl. Phys.* **68**, 5283 (1990).
17. J. Karpinski, E. Kaldis, E. Jilek, S. Rusiecki, and B. Bucher, *Nature* **336**, 660 (1988).